



SEISMIC PERFORMANCE OF REINFORCED CONCRETE CORNER BEAM-COLUMN JOINT SUBJECTED TO BI-DIRECTIONAL LATERAL CYCLIC LOADING

K. Kitayama⁽¹⁾, H. Katae⁽²⁾

⁽¹⁾ Professor, Tokyo Metropolitan University, kitak@tmu.ac.jp

⁽²⁾ Structural Engineer, PS Mitsubishi Co.Ltd., h-katae@psmic.co.jp

Abstract

Seismic performance of a corner beam-column joint in reinforced concrete frames was studied by testing two three-dimensional corner beam-column subassembly specimens without slabs under constant column axial load and bi-directional lateral cyclic load reversals. A column-to-beam flexural strength ratio was varied from 1.4 to 2.3 by changing the magnitude of column axial load. Although a sufficient margin to prevent shear failure was provided to a beam-column joint in the test, subassembly specimens failed in joint hinging after beam and column longitudinal bars and joint hoops yielded. The ultimate joint hinging capacity of a corner joint under bi-directional lateral loading was enhanced by column compressive axial load, and can be estimated based on the new mechanism proposed by Kusuhara and Shiohara.

Keywords: Reinforced concrete; Corner beam-column joint; Bi-directional loading; Joint failure; Seismic performance

1. Introduction

A new mechanism of joint hinging was proposed by Shiohara [1], a professor at the University of Tokyo, Japan, for a beam-column joint in reinforced concrete (R/C) moment-resisting frames. The joint hinging mechanism is observed in laboratory tests when an ultimate flexural capacity of a column section is close to that of a beam section in a R/C unit frame. A joint hinging model proposed by Kusuhara and Shiohara [2] is shown in Fig.1 for a plane exterior beam-column joint. An exterior beam-column subassembly is divided into three elements; an upper column, a lower column and a beam. Each element rotates like a rigid body as shown in Fig.1, forming a principal diagonal crack along a diagonal compression strut in a joint and a short diagonal crack developing from a reentrant corner in a tension side.

Recent experimental studies to verify the joint hinging mechanism have been conducted using 2D plane interior and exterior beam-column subassembly specimens. There are, however, few tests which use 3D beam-column-joint subassemblies with orthogonal beams to each other which frame into a column such as a corner beam-column joint. For corner columns in actual R/C buildings, a loss of capacity to sustain column axial load resulting from severe damage to a corner joint led to partial story collapse of the building by past earthquakes, for example, Guam Island Earthquake in 1993 as shown in Photo.1. An ultimate flexural capacity of a corner column frequently decreases during an earthquake because an axial load to a corner column cyclically increases and decreases by change of direction of lateral loads induced by earthquake excitations. Therefore, it is of great importance to investigate earthquake resistant performance of a corner beam-column joint subjected to tri-directional earthquake loading.

Therefore seismic performance of a corner beam-column joint in R/C frames was studied by testing two three-dimensional beam-column subassembly specimens without slabs under both constant column axial load and bi-directional lateral cyclic load reversals.

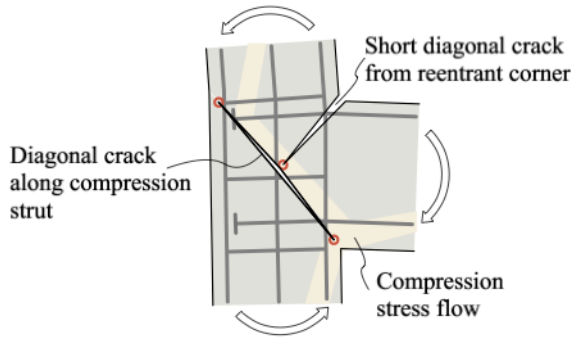


Fig. 1 – Joint hinging model at exterior joint [2]

Photo. 1 – Failure of corner beam-column joint by Guam Island Earthquake in 1993

2. Outline of test

2.1 Specimens

Two half-scale 3D corner beam-column subassemblage specimens without slabs, removed from a 3D frame by cutting off the beams and columns at arbitrarily assumed inflection points, were tested. A configuration of specimens, section dimensions and reinforcement details are shown in Fig.2. Properties of specimens and material properties of concrete and steel are listed in Table 1 and 2 respectively. The length from a center of the column to a support of the beam end was 1600 mm. The height from a center of the beam to the loading point at the top of the column or to the bottom support was 1200 mm respectively.

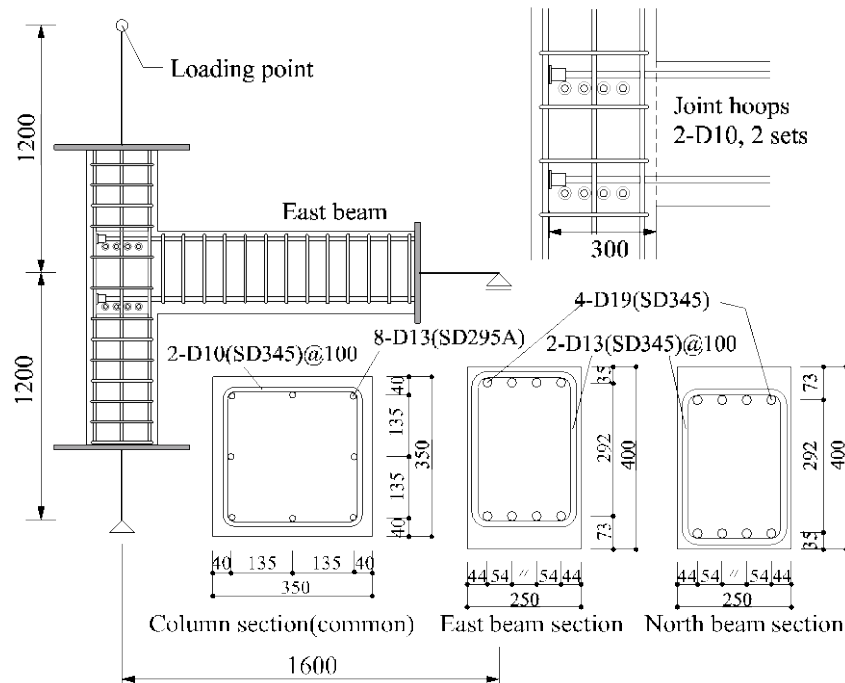


Fig. 2 – Details of specimens

Table 1 – Properties of specimens

Specimen		K2	K3
East and North beams	Width x Depth	250 x 400 mm	
	Longitudinal bars	Top and Bottom ; 4-D19	
	Stirrups	2-D13(SD345)@100	
Column	Width x Depth	350 x 350 mm	
	Longitudinal bars	8-D13(SD295A)	
	Hoops	2-D10@100	
Joint hoops		2-D10, 2 sets	
Column axial load (axial stress ratio)		260kN (0.04)	770kN (0.12)
Story shear force at ultimate beam flexural capacity (predicted)	Max.	74.9kN	75.9kN
	Min.	64.9kN	65.1kN
Story shear force at joint hinging capacity (predicted)	Max.	70.4kN	88.7kN
	Min.	60.0kN	82.0kN
Column-to-beam flexural strength ratio	Max.	1.4	2.3
	Min.	0.8	1.5
Joint shear redundancy ratio	under uni-directional loading	1.6	
	under bi-directional loading	1.1	

* Ultimate capacities are varied depending on loading directions.

Table 2 – Properties of materials

(a) Steel	Yield strength N/mm ²	Tensile strength N/mm ²	Yield strain %	Fracture strain %	(b) Concrete	Compressive strength N/mm ²	Tensile strength N/mm ²	Strain at comp. str. %	Young's modulus * ×10 ³ N/mm ²
D10(SD345)	393	546	0.19	17.0	SpecimenK2	50.5	3.4	0.23	31.1
D13(SD295A)	379	530	0.18	18.2	SpecimenK3	52.2	4.1	0.23	31.8
D13(SD345)	375	565	0.18	16.7					
D19(SD345)	394	568	0.19	18.2					

* Secant modulus at one-third of compressive strength

The magnitude of column compressive axial load was chosen as a test parameter; e.g., 260 kN corresponding to a column axial stress ratio of 0.04 for Specimen K2 and 770 kN corresponding to the ratio of 0.12 for Specimen K3. A column-to-beam flexural strength ratio was varied from 1.4 for Specimen K2 to 2.3 for Specimen K3 by changing the magnitude of column compressive axial load.

Section dimensions and reinforcement arrangement for beams and columns were common for two specimens. The column with a square cross section of 350 mm width had longitudinal bars of 8-D13(SD295A) and hoops of 2-D10(SD345) at center-to-center spacing of 100 mm. The beam had width of 250 mm and depth of 400 mm with longitudinal bars of 4-D19(SD345) at a top and a bottom respectively of the section and stirrups of 2-D13(SD345) at center-to-center spacing of 100 mm. A ratio of the total amount of column longitudinal bars to a column gross sectional area was 0.83 % and a joint-hoop-ratio was 0.28 %, which almost correspond to the lower bound required by Japanese Building Standard Law or seismic provisions. Beam longitudinal reinforcement was mechanically anchored by an end plate within joint core concrete with a horizontally projected length of 300 mm corresponding to 0.86 times the column depth. Concrete compressive strength was

approximately 50 N/mm². A joint shear redundancy ratio of 1.6 to a joint shear strength estimated by Architectural Institute of Japan provisions was provided to a corner beam-column joint in the test to prevent joint shear failure.

2.2 Loading apparatus and instrumentation

A loading apparatus is shown in Fig.3. Beam ends were supported by horizontal rollers, while a bottom of the column was supported by a universal joint. The reversed cyclic horizontal load and the constant axial load were applied at a top of the column through a tri-directional joint by three oil jacks. Rotation around a vertical axis in the column was prevented by a steel pantagraph placed in a horizontal plane. Specimens were controlled by a story drift angle for a loading cycle of 0.25 %, 0.5 %, 1 %, 1.5 %, 2 %, 3 % and 4 %. The story drift angle was defined as a story drift divided by a height of the column; 2400 mm.

Loading paths at a top of the column under bi-directional lateral load reversals are shown in Fig.4. The column top moves on a square in the horizontal plane. For a first loading cycle, after a prescribed drift was given to the top of the column from the origin point O to the point A in Fig.4 (a) to the west direction, a loading path depicts a counterclockwise square from points A to I, and then the column top goes back to the origin point O. For a second loading cycle, a loading path depicts a clockwise square from points J to R in Fig.4 (b). For all bi-directional lateral loading cycles, at first the lateral force in one direction was applied and then that in the other direction was applied while keeping the story drift in one direction constant.

Lateral forces, column axial load and beam shear forces were measured by load-cells. Story drift, beam and column deflections, and local displacement of a beam-column joint were measured by displacement transducers. Strains of beam and column longitudinal bars and joint hoops were measured by strain gauges.

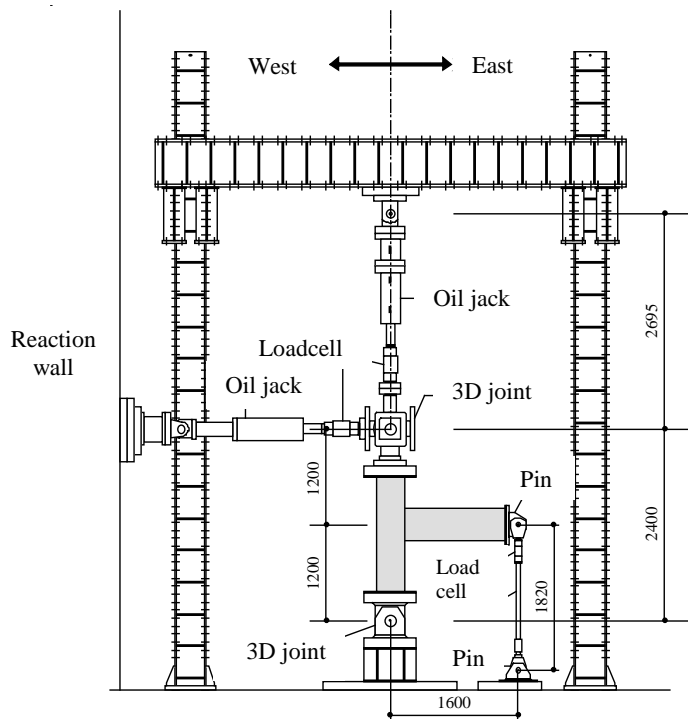


Fig. 3 – Loading apparatus

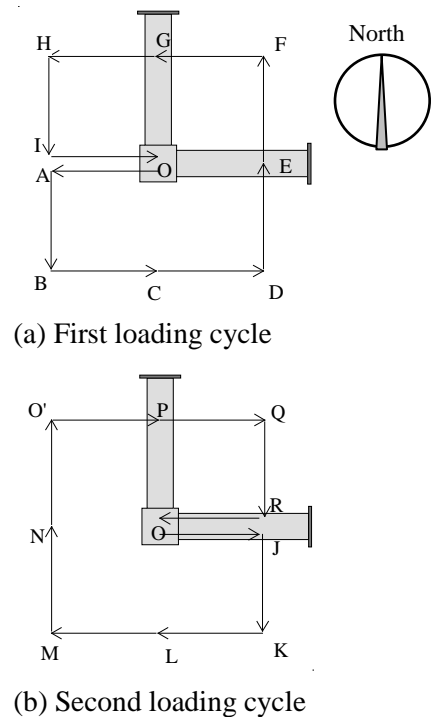


Fig. 4 – Loading Paths at top of column

3. Test results

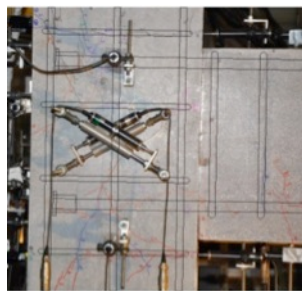
3.1 General observations

Crack patterns and damage conditions on the south surface are shown in Photo.2 at a story drift angle of 1 % and 2 %. Flexural cracks occurred at beam critical sections for two specimens at a story drift angle of 0.2 %. Principal diagonal cracks occurred in a beam-column joint and beam longitudinal bars and joint lateral hoops yielded during a loading cycle with a story drift angle of 1 % for two specimens. Column longitudinal bars yielded at a story drift angle of 0.9 % for Specimen K2 with a column axial stress ratio of 0.04 and 1.5 % for Specimen K3 with a column axial stress ratio of 0.12 respectively. Almost all longitudinal bars in beams and a column yielded at both the vertical or horizontal critical section and a point crossing a short diagonal crack which developed from a reentrant corner shown in Fig.1.

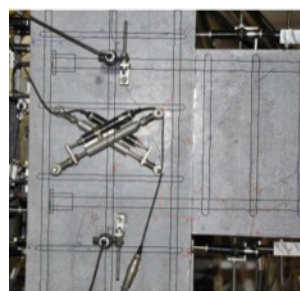
Damage in a joint panel for Specimen K3 with a column axial stress ratio of 0.12 was mitigated up to a story drift angle of 1.5 % comparing with Specimen K2 with a column axial stress ratio of 0.04, but progressed abruptly during a loading cycle with a story drift angle of 2 %. Core concrete in a joint region spalled off and column longitudinal bars buckled within a joint at a story drift angle of 3 % for Specimen K2 and 2 % for Specimen K3 respectively. Column bar buckling was caused by concrete crushing in beam-column joint core and inferior confining action due to a little amount of joint lateral hoops and column longitudinal bars.

Judging from these observations and the fact that the peak lateral-load carrying capacity did not attain to the ultimate shear capacity of a beam-column joint obtained by AIJ provisions, a joint failed eventually in not joint shear but joint hinging for two specimens. Beam ultimate flexural capacity for Specimen K3 was, however, at first developed at column faces as mentioned later.

Damage in a beam-column joint surface without framing beams was heavier than that with framing beams as shown in Photo.3. This indicates that beams framing into a joint panel contributed to mitigating damage to the joint due to its confining action.



(a-1) Specimen K2

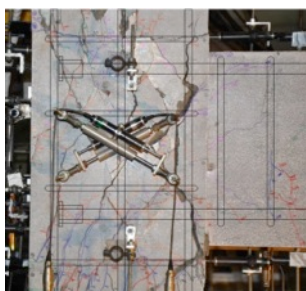


(a-2) Specimen K3



(a) Outer surface

(a) Crack patterns at story drift angle of 1 %



(b-1) Specimen K2



(b-2) Specimen K3



(b) Inner surface

(b) Crack patterns at story drift angle of 2 %

Photo. 2 – Crack patterns and damage conditions

Photo. 3 – Damage conditions for Specimen K3

3.2 Relationship between story shear and drift

The story shear force - story drift relations are shown in Fig.5 in the east-west and north-south directions. The story shear force was computed from moment equilibrium between measured beam shear force and the horizontal force at the loading point on a top of the column. Peak story shear forces and story drift angles when reaching the peak story shear force obtained by the tests are summarized in Table 3 with predicted ultimate capacities of a beam and a joint. The ultimate beam flexural capacity was computed by a section analysis assuming that a plane section remains plane, indicated by a horizontal solid line in Fig.5. The joint hinging capacity was evaluated according to a proposed method by Kushihara and Shiohara [2] based on the failure mechanics in a beam-column joint shown in Fig.1, indicated by a horizontal dotted line in Fig.5.

Hysteresis loops exhibited a little pinching shape for Specimen K2 with a column axial stress ratio of 0.04 (a column-to-beam flexural strength ratio of 1.4). In contrast, those showed a fat spindle shape for Specimen K3 with a column axial stress ratio of 0.12 (a column-to-beam strength ratio of 2.3), showing a more amount of energy dissipation. This was caused by restraint of diagonal crack opening in a joint due to large column axial load in Specimen K3.

Peak story shear capacity in uni-directional loading toward the west direction was 6 % lower than the predicted ultimate beam flexural capacity, but reached the joint hinging capacity for Specimen K2. Peak story shear capacity during bi-directional loading in the north-south direction, however, did not reach even the joint hinging capacity, being 20 % or 26 % lower than the joint hinging capacity or the ultimate beam flexural capacity respectively. This resulted from joint hinging failure under bi-directional loading, where the orbit of a story shear resistance depicted a part of an ellipse on a coordinate surface of the EW-NS direction story shear forces as mentioned later. The story shear capacity for Specimen K2 decreased by 25 % at a story drift angle of 3 % due to concrete crushing and column bar buckling within a joint region.

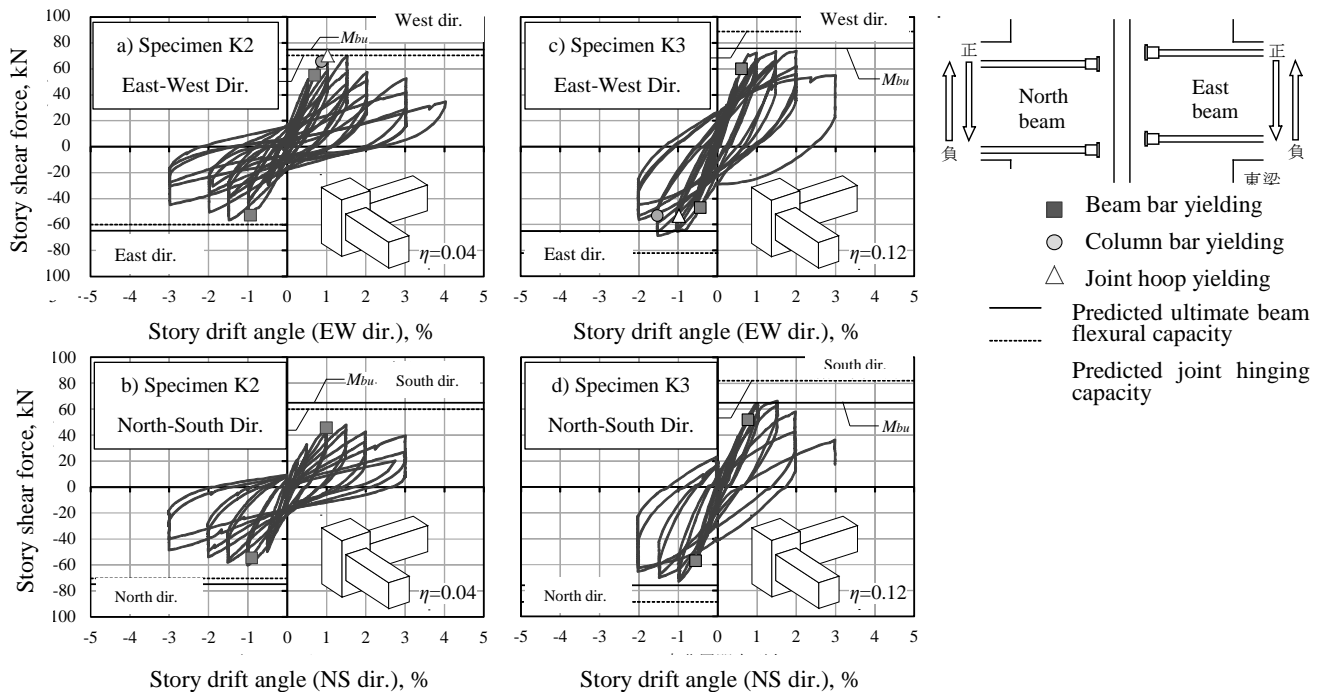


Fig. 5 – Story shear force - story drift angle relations

Table 3 – Peak story shear forces and story drift angles at peak story shear force

Specimen			K2	K3
Peak story shear force obtained by tests, kN	EW direction	Positive loading	70.3 (1.03%)	73.7 (2.00%)
		Negative loading	56.6 (1.48%)	68.6 (1.52%)
	NS direction	Positive loading	48.0 (1.50%)	66.3 (1.52%)
		Negative loading	60.2 (1.01%)	73.1 (0.99%)
Story shear force at predicted ultimate beam flexural capacity, kN	EW direction	Positive loading	74.9	75.9
		Negative loading	64.9	65.1
	NS direction	Positive loading	64.9	65.1
		Negative loading	74.9	75.9
Story shear force at predicted joint hinging capacity, kN	EW direction	Positive loading	70.4	88.7
		Negative loading	60.0	82.0
	NS direction	Positive loading	60.0	82.0
		Negative loading	70.4	88.7
Story shear force at predicted ultimate joint shear capacity in NS direction, kN			117.1	119.9

* A number in parentheses means a story drift angle in unit of % at peak story shear force.

Peak story shear capacity during uni- or bi-directional loading for Specimen K3 attained to 0.96 to 1.05 times the predicted ultimate beam flexural capacity. This indicates that beams developed almost fully its flexural capacity even during bi-directional loading. Damage concentrated on a joint region after loading point B shown in Fig.4 at a story drift angle of 2 %, resulting in severe crushing of joint core concrete and column bar buckling. Vertical axial deformation in a joint begun to shorten during a loading cycle with a story drift angle of 3 %. This shows symptom of a loss of axial load capacity. Thus the test for Specimen K3 was terminated.

4. Discussions

4.1 Diagonal crack width in joint

Widths of a principal diagonal crack along a main compression strut in a joint are shown in Fig.6. Those were measured by a crack-gauge under bi-directional loading at a story drift angle of 2 % located at both loading point F and point G at a EW directional story drift of zero as shown in Fig.4 (a). Note that a NS directional story drift was kept constant during loading point F to G, sustaining some story shear force in the north-south direction. Points where crack widths were measured are shown in Fig.7; a principal diagonal crack crosses a center axis of the column at point “a” and crosses another diagonal crack generated by a reversed loading at point “b”.

Maximum crack width for Specimen K3 was 1.3 mm at a loading point F subjected to peak story shear force in the east-west direction and 0.9 mm at loading point G at a EW directional story drift of zero, both at the measurement point “b”, which were less than half those at the point “a” for Specimen K2. The tendency that crack widths for Specimen K3 were smaller than that for Specimen K2 was observed in other loading points. This confinement of crack opening is attributed to compressive axial load to the column in Specimen K3 which was three times as large as that in Specimen K2.

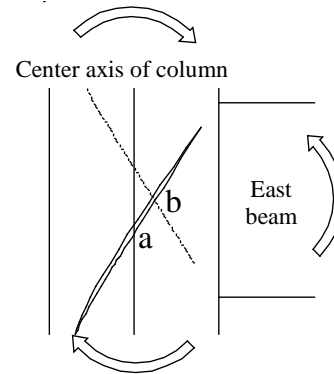
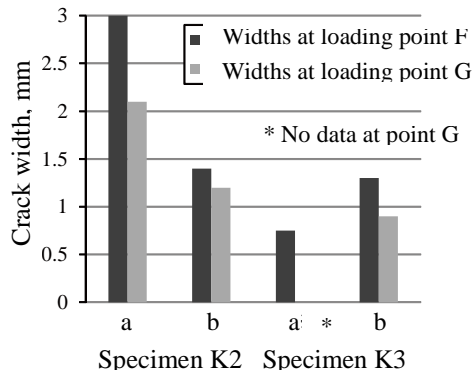


Fig. 6 – Principal diagonal crack widths in joint Fig. 7 – Measuring points of diagonal crack width

4.2 Biaxial interaction of story shear resistance

The orbit of a story shear resistance under bi-directional lateral loading in the first loading cycle is shown in Fig.8 at a story drift angle of 0.5 % before the occurrence of diagonal cracks in a joint, 1 % at diagonal cracking in a joint and 2 % at concrete crushing in a joint. The ultimate beam flexural capacity, the joint shear capacity and the joint hinging capacity each predicted by an aforementioned manner are shown in Fig.8. The ultimate flexural capacity surface of a beam shows two orthogonal lines and the biaxial interaction surface of the joint shear capacity or the joint hinging capacity does a circle or an ellipse respectively in Fig.8.

All the orbits of a story shear resistance under bi-directional loading remained inside a circle of the predicted joint shear capacity for two specimens. This indicates that a beam-column joint did not fail in shear.

The orbit of a story shear resistance for Specimen K2 depicted a rectangle under bi-directional loading at a story drift angle of 0.5 % since little damage occurred in a beam-column joint. The orbit, however, changed to a curved line at a story drift angle of 1 % because of joint damage. Then four peak points under bi-directional loading, i.e., points B, D, F and H in Fig.8 (a), were located on the ellipse line of the predicted joint hinging capacity.

The orbit of a story shear resistance for Specimen K3 with column axial load three times as large as Specimen K2 depicted a rectangle under bi-directional loading up to a story drift angle of 1 % since joint concrete suffered only slight damage. Peak story shear capacities especially at loading points B and D in Fig.8 (b) almost reached both the ultimate beam flexural capacity and the joint hinging capacity. Specimen K3 behaved dominantly in beam flexure and then reached the peak capacity because damage was slight in a beam-column joint at a story drift angle of 1 %. Just before loading point F at a story drift angle of 1 %, however, the story shear capacity in the east-west direction decreased due to the onset of joint hinging failure, which was attributed to reduction of axial load in the lower column at loading point F induced by vertical shear forces in both beams. After loading point F, damage to a joint grew remarkable with the increase in a story drift and a story shear resistance descended. Thus the orbit of a story shear resistance at a story drift angle of 2 % depicted curved lines and was located within the orbit at a story drift angle of 1 % for Specimen K3.

It is revealed that the ultimate capacity of corner beam-column joints under bi-directional lateral loading can be estimated based on the new mechanism of joint hinging failure proposed by Kusahara and Shiohara [2].

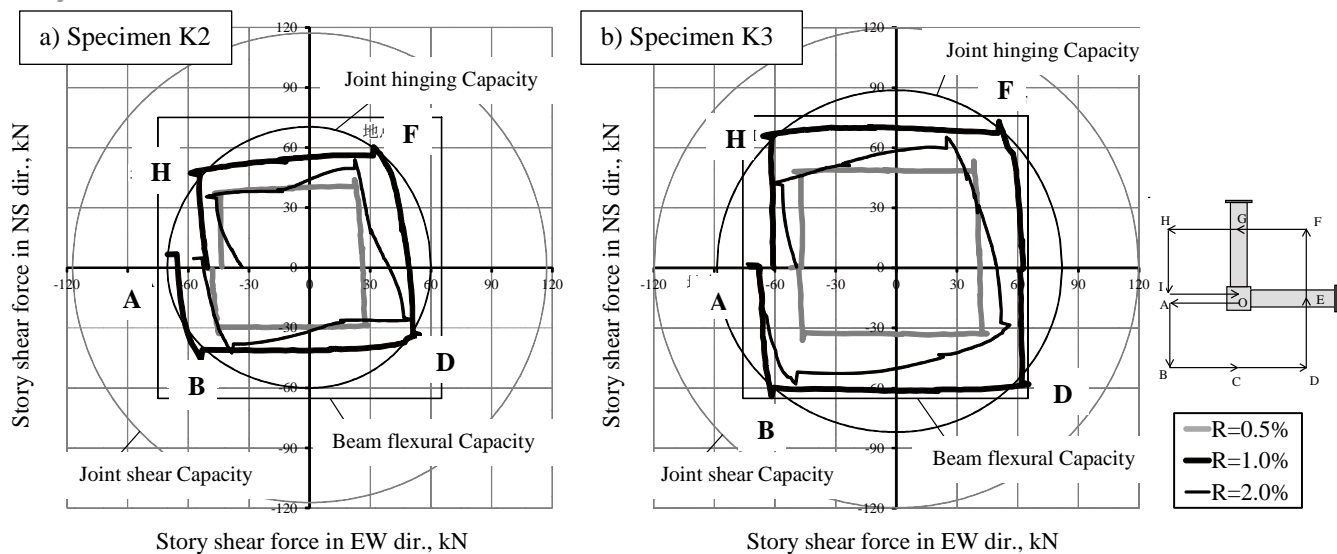


Fig. 8 – Orbit of story shear resistance under bi-directional loading

4.3 Story shear resultant force under bi-directional lateral loading

Envelope curves of relationship between a story shear resultant force and a story drift resultant angle under bi-directional loading from the origin point O to loading point C in a loading paths are shown in Fig.9. A story shear resultant force or a story drift resultant angle was obtained by the square root of sum of squares of story shear forces or story drift angles respectively in EW and NS directions.

A story shear force at loading point A reached the peak value of 70.6 kN at a story drift angle of 1 % for Specimen K2. During bi-directional loading from loading point A to B, a story shear resultant force remained to be almost constant; 70.6 kN at loading point B in Fig.9 (a). This was caused by a phenomenon that a beam-column joint started to fail in joint hinging at loading point A and the orbit of a story shear resistance under bi-directional loading depicted a part of an ellipse as shown in Fig.8 (a).

In contrast, flexural yielding for Specimen K3 occurred in an east beam at a story drift angle of 0.8 % and stiffness was degraded shown in Fig.9 (b). Under bi-directional loading from loading point A to B, a north beam yielded in flexure and a story shear resultant force increased to 89.0 kN at loading point B, which was 23 % larger than that at loading point A; 72.3 kN.

A peak story shear resultant force obtained at loading point B exceeded the predicted joint hinging capacity, shown by horizontal dashed lines in Fig.9, for two specimens; the former was 8 % or 4 % larger than the latter for Specimen K2 or K3 respectively. A story shear resultant force for Specimen K3 declined heavily due to progressive failure in a beam-column joint after a story drift resultant angle of 2.8 %, leading to axial collapse of the subassembly. This should be noted for seismic design to R/C buildings when a little amount of column longitudinal bars and joint lateral hoops is provided according to the lower bound required by Japanese law or seismic provisions.

5. Conclusions

General findings taken from the study are summarized as follows.

- (1) Although a joint shear capacity margin of 1.6 estimated by AIJ seismic provisions was provided to a corner beam-column joint in the test to prevent shear failure, all joints failed severely by joint hinging under bi-directional lateral cyclic loading after beam and column longitudinal bars and joint hoops yielded.
- (2) Peak story shear force in the transverse direction under bi-directional loading was 0.74 times the ultimate beam flexural capacity computed by a section analysis for a corner beam-column subassembly with a column

axial stress ratio of 0.04 (a column-to-beam flexural strength ratio of 1.4). Beams did not develop fully their flexural performance due to joint hinging failure. In contrast, peak story shear force under bi-directional loading almost attained to the ultimate beam flexural capacity for a subassembly with a column axial stress ratio of 0.12 (a column-to-beam flexural strength ratio of 2.3), whereas lateral-load carrying capacity descended severely after the peak capacity, attributed to severe damage in a joint region.

(3) When column compressive axial load was increased from an axial stress ratio of 0.04 to 0.12, the ultimate joint hinging capacity for a corner joint computed as a resultant force of two orthogonal story shear forces under bi-directional lateral loading was enhanced to 1.2 to 1.4 times by large column axial load. A joint hinging capacity with an axial stress ratio of 0.12, however, decreased heavily after the peak capacity, leading to axial collapse of the subassembly. This should be noted for seismic design to R/C buildings when a little amount of column longitudinal bars and joint lateral hoops is provided according to the lower bound required by Japanese law or seismic provisions.

(4) The ultimate capacity of a corner beam-column joint under bi-directional lateral loading can be estimated based on the new mechanism of joint hinging proposed by Kusuhara and Shiohara if it is assumed that the orbit for two joint hinging capacities orthogonal to each other depicts an ellipse shape under bi-directional loading.

(5) Fatter hysteresis loops were observed under bi-directional lateral loading for a corner beam-column subassembly specimen with a column compressive axial stress ratio of 0.12 than that of 0.04, showing a more amount of energy dissipation. This was caused by restraint of diagonal crack opening in a joint due to large column axial load.

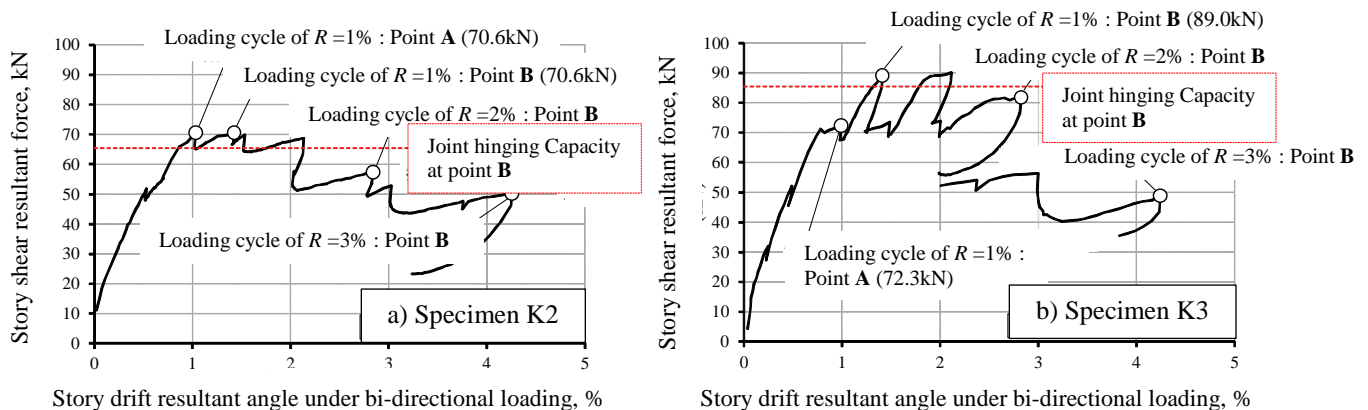


Fig. 9 – Story shear resultant force under bi-directional loading

6. Acknowledgements

The study described herein was sponsored by the Grant-in-aid for Scientific Research (B) of Japan Society for the Promotion of Science (Principal researcher : H. Shiohara, professor of the University of Tokyo, Japan). Authors would like to express their gratitude to Prof. Shiohara for his valuable advice, Dr. T. Endo, former assistant professor of Tokyo Metropolitan University, for his assistance in conducting the tests and Tokyo Tekko Co. Ltd. for providing steel bars.

7. References

- [1] Shiohara H (2001): New model for shear failure of RC interior beam-column connections. *Journal of Structural Engineering*, Vol.127, No.2, February 2001, ASCE, 152-160.
- [2] Kusuhara F, Shiohara H (2013): Ultimate moment of reinforced concrete exterior beam-column joint. *Journal of Structural and Construction Engineering*, Vol.78, No.693, November 2013, AIJ, 1949-1958.